European Journal of Radiology 113 (2019) 188–197

Contents lists available at ScienceDirect

European Journal of Radiology

journal homepage: www.elsevier.com/locate/ejrad

Research article

Unresectable pancreatic ductal adenocarcinoma: Role of CT quantitative imaging biomarkers for predicting outcomes of patients treated with chemotherapy

Si-Hang Cheng[a,1], Yue-Juan Cheng[b,1], Zheng-Yu Jin[a], Hua-Dan Xue[a,*]

[a] Department of Radiology, Peking Union Medical College Hospital, Chinese Academy of Medical Sciences, Beijing 100730, China
[b] Department of Oncology, Peking Union Medical College Hospital, Chinese Academy of Medical Sciences, Beijing 100730, China

ARTICLE INFO

Keywords:
Unresectable pancreatic ductal adenocarcinoma
CT texture analysis
Survival
Chemotherapy

ABSTRACT

Objectives: The primary aim of this study was to determine if computed tomographic (CT) texture analysis measurements of the tumor are independently associated with progression-free survival (PFS) and overall survival (OS) in patients with unresectable pancreatic ductal adenocarcinoma (PDAC), including both unresectable locally advanced and metastatic PDAC, who were treated with chemotherapy.

Methods: After an institutional review board waiver was obtained, contrast material-enhanced CT studies in 41 patients with unresectable PDAC who underwent contrast-enhanced CT before chemotherapy between 2014 and 2017 were analyzed in terms of tumor texture, with quantification of mean gray-level intensity (Mean), entropy, mean of positive pixels (MPP), kurtosis, standard deviation (SD), and skewness for fine to coarse textures (spatial scaling factor (SSF) 0–6, respectively). The association between pretreatment and posttreatment texture parameters, as well as Δ value (difference between posttreatment and pretreatment texture parameters), and survival time was assessed by using Cox proportional hazards models and Kaplan-Meier analysis.

Results: Findings from the multivariate Cox model indicated that tumor size, tumor SD (HR, 0.942; 95% CI: 0.898, 0.988) and skewness (HR, 0.407; 95% CI: 0.172, 0.962) measurements with SSF = 3, and tumor SD (HR, 0.958; 95% CI: 0.92, 0.997) measurements with SSF = 4 were significantly and independently associated with PFS, while tumor size and tumor SD (HR, 0.928; 95% CI: 0.882, 0.976) measurements with SSF = 3 were significantly and independently associated with OS. None of the post-therapy texture parameters or Δ value had a significant association with OS or PFS in multivariate Cox regression models. Medium SD (SSF = 3) of more than 38.38 and coarse SD (SSF = 4) of more than 40.67 were associated with longer PFS after chemotherapy (for SSF = 3, median PFS was 10.0 vs 6.0 months [P = 0.024], and for SSF = 4, median PFS was 12.0 vs 6.0 months [P = 0.003]). SD of 38.38 or greater (SSF = 3) as a dichotomized variable was a significant positive prognostic factor for OS (median OS, 20.0 vs 9.0 months [P = 0.04]). Survival models that included a combination of pretreatment SD (SSF = 3) with tumor size, had the potential to perform better than SD alone, while having no statistical significance in this study (area under the ROC curve, 0.756 vs 0.715 [P = 0.066]).

Conclusions: Pretreatment CT quantitative imaging biomarkers from texture analysis are associated with PFS and OS in patients with unresectable PDAC who were treated with chemotherapy, and the combination of pretreatment texture parameters and tumor size have the potential to perform better in survival models than imaging biomarker alone.

1. Introduction

Pancreatic cancer has been reported to have increasing death rates in recent years, with a 5-year overall survival rate of only 3% [1]. It is the 4th leading cause of cancer death, with approximately 55,440 estimated new cases and 44,330 estimated deaths in the United States in 2018 [1]. Patients with pancreatic cancer tend to have advanced stages at presentation, and 53% of pancreatic cancers are diagnosed metastatic and 28% with locally advanced disease, with 5-year survival rates of 2% and 11%, respectively [2]. According to the National

* Corresponding author at: Department of Radiology, Peking Union Medical College Hospital, Chinese Academy of Medical Sciences, Shuaifuyuan No.1, Wangfujing Street, Dongcheng District, Beijing 100730, China.
E-mail address: bjdanna95@hotmail.com (H.-D. Xue).
[1] Si-Hang Cheng and Yue-Juan Cheng contributed equally to this work.

https://doi.org/10.1016/j.ejrad.2019.02.009
Received 15 November 2018; Received in revised form 4 February 2019; Accepted 10 February 2019

Comprehensive Cancer Network (NCCN) guideline, pancreatic cancer without metastasis is classified into resectable, borderline resectable and unresectable disease. Most patients present with unresectable locally advanced or metastatic disease that precludes curative resection. At the present time, the most widely accepted treatment approach for patients with advanced disease is chemotherapy, either gemcitabine given alone or combined with a platinum agent, erlotinib, or a fluoropyrimidine [2].

Patients with unresectable PDAC respond differently to chemotherapy. Part of these patients show poor response due to either nonresponding tumors or the increase in toxic effects and the risk of complications, which may lead to a delay in subsequent definitive therapy. Factors related to a poor response to chemotherapy are still unclear, therefore, it is quite important to find appropriate factors to identify patients who will not optimally benefit from chemotherapy, which could offer substantial clinical benefits.

There are a limited number of prognostic factors for locally advanced and metastatic pancreatic cancer. Baseline performance status, elevated CA 19-9 and gender are associated with overall survival in locally advanced pancreatic cancer [3]. In addition, Karnofsky performance status (KPS) score, presence of liver metastases, age and number of metastatic sites were independent prognostic factors of overall and progression-free survival for patients with metastatic pancreatic cancer [4]. Other potential biomarkers associated with survival include genetic profiles and the expression profiles of messenger RNA and proteins and receptors in the tumor such as Decoy receptor 3 [5–8]. Most of these biomarkers are investigated based on experiments with tissue sampling, which needs accurate biopsy. However, tissues from biopsy specimen only account for a small part of the tumor, which cannot represent tumor characteristics comprehensively. Accordingly, easily accessible noninvasive methods that can reflect tumor heterogeneity are urgently-needed.

Angiogenesis in cancer produces disorganized and leaky blood vessels, resulting in the formation of hypoxic and acidic microenvironment within the tumor. This leads to spatial and temporal vascular anomalies that contribute to tumor heterogeneity, as well as to different chemotherapy responses [9]. CT texture analysis, a novel imaging post-processing tool, can reflect tumor heterogeneity through analyzing the distribution of pixel intensities in CT images and identifying relationships among those intensities. This may reveal subtle differences imperceptible to the naked eye, thereby compensating for the limitations of conventional CT [10–13]. CT texture analysis relies on objective computer-aided evaluation of gray-level patterns within lesions to assess tumor heterogeneity quantitatively in terms of numerous relevant parameters, which has been used in the prediction of various cancer prognosis [14]. In locally advanced rectal cancer, CT texture features have been associated with better neoadjuvant chemoradiotherapy response and higher disease-free survival [15]. In pancreatic adenocarcinoma, CT-derived texture features of dissimilarity and inverse normalized differences may be promising prognostic imaging biomarkers of overall survival in patients undergoing surgical resection with curative intent [16].

To date there have been few studies investigating the potential of texture analysis in unresectable pancreatic ductal adenocarcinoma (PDAC), including both unresectable locally advanced or metastatic PDAC in survival prediction setting, particularly for the identification of patients with poor prognosis after chemotherapy, which may help avoid unnecessary drug toxicity and cost and allow the choice of an alternative treatment regimen that might improve clinical outcome. The primary aim of this study was to determine if CT texture analysis measurements of the tumor are independently associated with progression-free survival (PFS) and overall survival (OS) in patients with unresectable PDAC who were treated with chemotherapy.

2. Materials and methods

All of the authors had control of the data and information submitted for publication without conflict of interest.

2.1. Patient population

An institutional review board waiver was obtained for this retrospective study. Patients who received definitive chemotherapy for unresectable locally advanced or metastatic pancreatic cancer in a single tertiary center between January 2014 and January 2017 were identified from the oncology database. Only patients given a histologic diagnosis of PDAC with contrast-enhanced CT imaging less than 90 days before the start of chemotherapy were included in this study. Sixty patients were initially identified. Exclusion criteria were patients who had (a) received chemotherapy followed by surgery (eight patients, 13%); (b) recurrent or previously treated PDAC; (c) resectable or borderline resectable PDAC; (d) missing CT images (one patient, 2%); nonenhanced CT images of the pancreas (one patient, 2%); no baseline CT images before chemotherapy (nine patients, 15%); CT images with substantial motion artifact; or pretherapy CT imaging more than 90 days from the start of therapy or posttherapy CT imaging more than 90 days from the completion of chemotherapy; (e) received chemotherapy other than gemcitabine-based chemotherapy regimen. A total of 19 patients (32%) were excluded, leaving 41 patients whose data were available for survival for further analysis. Endoscopic ultrasound-guided fine-needle biopsy (EUS-FNB) had been performed for these patients before the start of chemotherapy (median cycles of chemotherapy, 4; range, 2–21). Tumor staging was performed according to the American Joint Committee on Cancer AJCC Cancer Staging Manual (8th edition), and N-stage definitions included the following: N0 = node negative, N1 = 1–3 nodes positive for metastatic disease, N2 ≥ 4 nodes positive for metastatic disease [17]. All patients underwent clinical follow-up as per institutional protocol. Data in patients known to be alive at the time of their last follow-up were censored in the survival analysis.

2.2. Image acquisition and analysis

All images were acquired in the Department of Radiology at our hospital. All the scans were done on 128-detector CT scanners (Siemens SOMATOM Definition Flash, Siemens Healthcare, Forchheim, Germany). The scanning parameters were as follows: tube voltage, 120kVp; tube current, 150 mAs; gantry rotation time, 0.5 s; table increment 46.8 mm per rotation; matrix 512 × 512. Images were routinely reconstructed with 5.0 mm slice thickness and 5.0 mm intervals. Non-ionic contrast media (Ultravist, 370 mg of iodine per milliliter, Schering, Berlin, Germany) were injected with 1.5 mL per kilogram of body weight at a rate of 3.0 mL/s using an automatic power injector. Bolus tracking was applied, and the pancreatic arterial phase (PAP) scan was started with a 5 s delay from aortic enhancement of 100 HU. The portal venous phase (PVP) scan was started 30 s after the PAP phase imaging acquisition. The delayed phase was started 90 s after the PAP phase. According to previous studies, CT images of portal phase were used for texture analysis [16,18–20].

All imaging measurements were made by a fellowship-trained academic radiologist with 20 years of abdominal imaging experience and 5years of texture analysis experience, who was blinded to clinical and survival data. The longest dimension of the tumor was measured using a commercial image viewing software (Centricity, GE Medical Systems, Milwaukee, WI, USA). Texture analysis measurements of the tumor were made by using TexRAD commercial research software (TexRAD Ltd, www.texrad.com, part of Feedback Plc, Cambridge, UK) to draw a region of interest (ROI) around the peripheral margin of the tumor on contiguous 5-mm CT images. Air, dense calcification, metal, and streak artifacts were excluded from the ROI. The TexRAD software quantifies

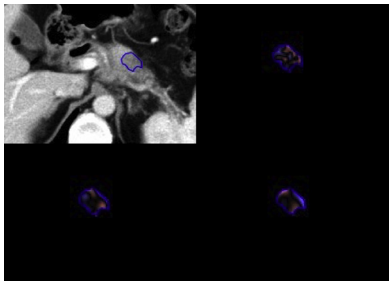

Fig. 1. Example of texture analysis maps after filtration at spatial scaling factors (SSF) of 2, 4, and 6 for a patient with pancreatic body adenocarcinoma.

various texture analysis parameters in a user-selected ROI on the CT images before and after application of various Laplacian of Gaussian spatial band-pass filters (Fig. 1). The scale was selected by altering the filter value between 0 and 6; filter value 0 indicated absence of filtration (spatial scaling factor (SSF) = 0); 2 indicated fine texture (SSF = 2, features of 4 pixels or 1.2 mm in width), 3 and 4 indicated degree of medium textures (SSF = 3 or 4, features of 6 and 8 pixels or 1.8 and 2.4 mm in width, respectively), 5 and 6 indicated coarse texture (SSF = 5 or 6, features of 10 and 12 pixels or 3 and 3.6 mm in width, respectively). This resulted in derived CT texture images displaying imaging features at different spatial scales in the region of interest (Fig. 1). The CT texture parameter measured in this study included (1) mean gray-level intensity (Mean, brightness); (2) standard deviation (SD, spread of distribution); (3) entropy (irregularity or complexity of pixel intensity in space); (4) mean of positive pixels (MPP); (5) skewness (symmetry of the pixel intensity distribution); (6) kurtosis (sharpness or pointedness of the pixel intensity distribution).

2.3. Statistical analysis

SPSS software (SPSS for Mac, version 20, SPSS Inc., SPSS, Chicago, IL) was used for statistical analysis. Descriptive statistics were expressed as numbers and percentages for categorical variables and mean ± standard deviation or medians with interquartile range for continuous variables. Univariate analyses using the Cox proportional hazards model were performed to assess the independent effects of CT texture analysis measurements of the tumor on PFS and OS. PFS time was measured from the date of the therapy to the date of progression or the date of the last clinical follow-up. OS time was defined as the time from start of therapy until either death from any cause (event) or the date that the patient was last known to be alive (censored). Mean values for significant texture parameter were used (only for normally distributed texture parameter, if not, median values were used) as threshold levels to dichotomize patients for Kaplan-Meier survival analysis, and comparisons between groups were performed by using the log-rank test. Significant univariate prognostic factors were adjusted for clinically important confounders such as tumor size, sex and age with the multivariate Cox proportional hazards model. Results from the Cox proportional hazards models were reported as hazard ratios (HRs), with 95% confidence intervals (CIs) and *P* values. Receiver operating characteristic (ROC) curve analysis was performed to compare the accuracy of survival models in assessing the chance of survival by using texture parameters alone and the combination of maximal tumor diameter, respectively, and texture parameters against morphologic assessment only. Areas under the ROC curve (AUCs) were obtained to measure the performance and discrimination of each survival model in assessing the chance of survival. Comparisons between AUCs were performed by using the DeLong test [21]. Two-sided *P* values less than 0.05 were considered to indicate a significant difference.

Table 1
Patient and Tumor Characteristics.

Characteristic	Value
Age (y)	59.7 ± 9.6 (34-76)*
Sex	
Male	26 (63)
Female	15 (37)
CA 19-9 (U/mL)	629.5 (1568.1) [0.6 to 103,641.0]†
Tumor location	
Head	16 (39)
Neck	6 (15)
Body/tail	19 (46)
Histologic grade	
Well	1 (3)
Moderate	18 (44)
Poor	22 (53)
Tumor size (cm)	3.7 ± 1.9 (1.3-8.1)*
Tumor attenuation (HU)	53.8 ± 17.3 (16.7-94.7)*
T stage	
T1	4 (10)
T2	6 (14)
T3	9 (22)
T4	22 (54)
N stage	
N0	12 (29)
N1	15 (37)
N2	14 (34)
M stage	
M0	17 (42)
M1	24 (58)
Overall stage	
III	17 (42)
IV	24 (58)
Locally advanced	17 (42)
Metastatic	24 (58)
Metastatic site	
Liver	19 (43)
Lung	4 (10)
Bone	2 (5)
Peritoneum	3 (7)
Number of liver metastatic lesions	
≤5	11
> 5	8
Chemotherapy	
Gemcitabine alone	1 (2)
Gemcitabine + tegafur	40 (98)
Median progression-free survival (m)	6.0 (7.0) [1.5 to 16.0]†
Median overall survival (m)	10.0 (9.5) [1.5 to 27.0]†

Note.—Unless otherwise indicated, data are number of patients, with percentages in parentheses.

* Data are mean ± standard deviation, with range in parentheses for normally distributed data.

† Data are median with interquartile range in parentheses and minimum and maximum in brackets for skewed data.

3. Results

The majority of patients (24 [58%] of 41) had stage IV disease, and 42% (17 of 41) of patients had stage III disease. Nineteen patients had liver metastases, of which 11 had more than 5 metastatic lesions. Metastatic sites in lung, bone and peritoneum were also found. Most patients had tumors in the body and tail of the pancreas (Table 1).Most patients (40 [98%] of 41) received concurrent gemcitabine and tegafur chemotherapy, and only one patient received gemcitabine single-agent chemotherapy. National Comprehensive Cancer Network (NCCN) criteria for CT resectability of pancreatic cancer was used to evaluate resectability before and after treatment, and no patients were found to be resectable before the end of follow-up. The median time from the pretreatment CT study to the start of chemotherapy was 23 days (range, 0–36 days). The median time from the completion of chemotherapy to the posttreatment CT study were 39 days (range, 14–77 days). Median PFS and OS for the entire cohort were 6.0 months (range, 1.5–16.0

Table 2
Tumor CT Texture Analysis Measurements by Spatial Scaling Factor (SSF).

SSF	CT texture Parameters					
	Entropy	Mean Intensity	Standard Deviation	Skewness	Kurtosis	Mean of positive pixels
0	4.06 ± 0.22 (3.55 to 4.61)	57.07 ± 17.11 (32.04 to 96.63)	15.18 (3.31) [10.27 to 27.77]*	0.07 ± 0.26 (-0.49 to 0.69)	0.08 (0.52) [-0.39 to 1.48]*	57.29 ± 16.91 (32.94 to 96.63)
2	4.81 ± 0.21 (4.3 to 5.21)	−4.08 (14.02) [-46.2 to 14.34]*	37.79 ± 7.52 (23.48 to 53.22)	0.1 ± 0.29 (-0.5 to 0.79)	0.12 (0.7) [-0.71 to 1.58]*	28.64 ± 6.17 (14.30 to 44.94)
3	4.79 ± 0.21 (4.37 to 5.16)	−5.86 (21.53) [-68.16 to 25.53]*	38.38 ± 9.05 (20.98 to 57.4)	0.25 (0.53) [-0.54 to 1.41]*	0.24 (0.93) [-0.76 to 3.33]*	29.37 ± 8.83 (14.27 to 49.64)
4	4.82 ± 0.26 (4.38 to 5.31)	−7.41 (25.64) [-84.35 to 32.85]*	40.67 ± 11.45 (21.11 to 73.57)	0.15 ± 0.46 (-1.02 to 1.1)	0.11 (1.11) [-1.1 to 3.49]*	31.51 ± 10.45 (13.58 to 57.36)
5	4.83 ± 0.29 (4.31 to 5.43)	−5.77 (32.42) [-92.77 to 39.51]*	38.3 (17.4) [23.75 to 84.79]*	0.09 ± 0.58 (-1.15 to 1.18)	−0.16 (1.23) [-1.18 to 5.7]*	33.07 ± 12.21 (8.93 to 65.31)
6	4.83 ± 0.32 (4.23 to 5.43)	−7.84 ± 27.2 (-93.71 to 46.31)	40.42 (21.32) [23.57 to 89.89]*	0.08 ± 0.61 (-1.14 to 1.57)	−0.44 (1.25) [-1.44 to 7.95]*	34.6 ± 14.08 (5.75 to 67.5)

Note.—Unless otherwise indicated, data are mean ± standard deviation, with range in parentheses for normally distributed data.
* Data are median with interquartile range in parentheses and minimum and maximum in brackets for skewed data.

months) and 10.0 months (range, 1.5–27.0 months), respectively. Nine (22%) of the 41 patients were non-progressive for PFS and eighteen (44%) were alive for OS, thus censored data were analyzed. For PFS, the median follow-up for these 9 patients was 4.5 months (range, 1.5–14.0 months) compared with the median follow-up of 6.0 months (range, 1.5–16.0 months) in patients who progressed. For OS, the median follow-up for these 18 patients was 11.0 months (range, 1.5–26.5 months) compared with the median follow-up of 9.0 months (range, 2.5–27.0 months) in patients who died.

Table 2 lists the summary statistics of the CT texture analysis measurements of the tumor from the baseline pre-chemotherapy contrast-enhanced CT study with various spatial filters. Results from univariate Cox regression analysis evaluating the association of baseline clinical parameters and PFS and OS are shown in Table 3. **For univariate analysis, *P* value less than 0.1 was considered to be significant, which could avoid omitting potential positive factors.** Both age (HR, 0.963; 95% CI: 0.921, 1.006) and tumor size (HR, 1.348; 95% CI: 1.081, 1.681) were associated with PFS, while only tumor size (HR, 1.35; 95% CI: 1.092, 1.669) was significantly associated with OS. No difference was found between patients with locally advanced cancer and patients with already metastatic disease in terms of prognosis. Results from univariate Cox regression analysis evaluating the association of baseline, post-treatment tumor CT texture analysis measurements and Δ value (difference between posttreatment and pretreatment texture parameters) with various spatial filters and PFS and OS, respectively, are shown in Tables 4–6.

Table 7 shows that, after adjustment for age, sex, and tumor size, both baseline tumor SD (HR, 0.942; 95% CI: 0.898, 0.988) and skewness (HR, 0.407; 95% CI: 0.172, 0.962) measured with SSF = 3, and tumor SD (HR, 0.958; 95% CI: 0.92, 0.997) measured with SSF = 4, were associated with PFS. Tumor SD (HR, 0.928; 95% CI: 0.882, 0.976) measured with SSF = 3 was significantly associated with OS. Findings from the multivariate Cox model indicated that tumor size, tumor SD and skewness measurements with SSF = 3, and tumor SD measurements with SSF = 4 were significantly and independently associated with PFS, while tumor size and tumor SD measurements with SSF = 3 were significantly and independently associated with OS (Table 7). However, none of the post-therapy texture parameters or Δ value had a significant association with OS or PFS in multivariate Cox regression models.

Medium SD (SSF = 3) of more than 38.38 and coarse SD (SSF = 4) of more than 40.67 were associated with longer PFS after chemotherapy (for SSF = 3, median PFS was 10.0 vs 6.0 months [P = 0.024], and for SSF = 4, median PFS was 12.0 vs 6.0 months [P = 0.003]) (Fig. 2a, b). SD of 38.38 or greater (SSF = 3) as a dichotomized variable was a significant positive prognostic factor for OS (median OS, 20.0 vs 9.0 months [P = 0.04]) (Fig. 2c). Skewness (SSF = 3) of 0.17 or greater as a dichotomized variable tended to be associated with longer PFS; nevertheless, no significant difference was detected (P = 0.061).

Morphologic assessment using maximal tumor diameter (tumor size) was significant survival prognostic factors for both PFS (HR, 1.348; 95% CI: 1.081, 1.681) and OS (HR, 1.35; 95% CI: 1.092, 1.669) from the results of multivariate Cox regression analysis. Kaplan-Meier analysis demonstrated significantly decreased PFS (P = 0.004) and OS (P = 0.002) in patients with tumor size of more than 3.73 cm (Fig. 3a, b).

In assessing the chance of OS, the survival models using the combination of pretreatment SD (SSF = 3) as continuous variables with tumor size had an AUC value of 0.756 (P = 0.005), while SD (SSF = 3) alone had an AUC value of 0.715 (P = 0.019). However, the combination of pretreatment SD (SSF = 3) and tumor size did not perform better than SD (SSF = 3) alone (P = 0.066) (Fig. 4). Similarly, survival models using the combination of pretreatment texture parameters and tumor size did not perform better than texture parameters alone in assessing the chance of PFS.

Table 3
Univariate Cox-Proportional Hazards Regression Analysis of Clinical Parameters for Progression-Free Survival and Overall Survival.

	Progression-Free Survival		Overall Survival	
Clinical Parameters	HR	P Value	HR	P Value
Age	0.963 (0.921, 1.006)	**0.091***	0.966 (0.925, 1.008)	0.114
Sex	0.778 (0.374, 1.618)	0.501	0.461 (0.18, 1.184)	0.108
CA 19-9	1.595 (0.76, 3.345)	0.217	1.333 (0.572, 3.11)	0.506
Tumor location				
Head/neck versus Body/tail	0.529 (0.245, 1.139)	0.104	0.578 (0.241, 1.384)	0.218
Tumor size	1.348 (1.081, 1.681)	**0.008***	1.35 (1.092, 1.669)	**0.006***
Tumor attenuation	0.996 (0.976, 1.017)	0.724	0.999 (0.973, 1.025)	0.917
T stage	–	0.872	–	0.962
N stage	–	0.728	–	0.508
M stage	1.263 (0.59, 2.704)	0.548	1.085 (0.453, 2.597)	0.855
Overall stage	1.263 (0.59, 2.704)	0.548	1.085 (0.453, 2.597)	0.855
Locally advanced versus metastatic	1.263 (0.59, 2.704)	0.548	1.085 (0.453, 2.597)	0.855
Liver metastasis	1.128 (0.548, 2.321)	0.743	0.76 (0.324, 1.784)	0.529

Note.—Data in parentheses are 95% confidence intervals.
* Indicates a significant difference ($p < 0.1$).

Table 4
Univariate Cox-Proportional Hazards Regression Analysis of Pre-Treatment Tumor CT Texture Parameters for Progression-Free Survival and Overall Survival.

	Progression-Free Survival		Overall Survival	
Spatial scaling factor (SSF)	HR	P Value	HR	P Value
No filtration				
Entropy	0.614 (0.107, 3.522)	0.585	0.947 (0.096, 9.355)	0.963
Mean intensity	0.997 (0.977, 1.017)	0.75	0.995 (0.969, 1.021)	0.685
Standard deviation	0.929 (0.834, 1.036)	0.186	0.926 (0.797, 1.076)	0.317
Skewness	0.28 (0.065, 1.203)	**0.087***	0.18 (0.032, 0.999)	**0.05***
Kurtosis	0.941 (0.417, 2.123)	0.884	0.577 (0.207, 1.612)	0.294
Mean of positive pixels	0.996 (0.975, 1.016)	0.683	0.994 (0.967, 1.021)	0.636
SSF = 2 (fine)				
Entropy	1.085 (0.205, 5.743)	0.924	1.657 (0.226, 12.17)	0.62
Mean intensity	1.015 (0.99, 1.044)	0.23	1.017 (0.983, 1.052)	0.324
Standard deviation	0.96 (0.912, 1.01)	0.112	0.952 (0.897, 1.011)	0.11
Skewness	0.223 (0.055, 0.898)	**0.035***	0.185 (0.04, 0.862)	**0.032***
Kurtosis	1.007 (0.571, 1.776)	0.982	1.017 (0.473, 2.186)	0.966
Mean of positive pixels	0.953 (0.895, 1.014)	0.13	0.938 (0.872, 1.009)	**0.085***
SSF = 3 (medium)				
Entropy	0.586 (0.103, 3.346)	0.548	0.448 (0.061, 3.306)	0.431
Mean intensity	1.009 (0.992, 1.026)	0.308	1.01 (0.988, 1.032)	0.378
Standard deviation	0.936 (0.893, 0.982)	**0.006***	0.928 (0.882, 0.976)	**0.004***
Skewness	0.364 (0.157, 0.84)	**0.018***	0.285 (0.099, 0.821)	**0.02***
Kurtosis	0.985 (0.691, 1.404)	0.933	1.101 (0.706, 1.717)	0.67
Mean of positive pixels	0.937 (0.893, 0.984)	**0.009***	0.927 (0.878, 0.979)	**0.006***
SSF = 4 (medium)				
Entropy	0.529 (0.133, 2.108)	0.366	0.442 (0.084, 2.331)	0.336
Mean intensity	1.006 (0.993, 1.019)	0.397	1.007 (0.99, 1.025)	0.415
Standard deviation	0.949 (0.912, 0.987)	**0.008***	0.944 (0.903, 0.988)	**0.012***
Skewness	0.576 (0.274, 1.211)	0.146	0.456 (0.179, 1.158)	**0.099***
Kurtosis	1.137 (0.754, 1.716)	0.54	1.444 (0.93, 2.242)	0.101
Mean of positive pixels	0.954 (0.918, 0.992)	**0.017***	0.945 (0.902, 0.99)	**0.017***
SSF = 5 (coarse)				
Entropy	0.773 (0.262, 2.281)	0.641	0.882 (0.223, 3.484)	0.858
Mean intensity	1.004 (0.993, 1.015)	0.514	1.005 (0.991, 1.02)	0.474
Standard deviation	0.965 (0.934, 0.997)	**0.034***	0.967 (0.931, 1.006)	**0.093***
Skewness	0.788 (0.426, 1.454)	0.445	0.645 (0.306, 1.357)	0.248
Kurtosis	1.193 (0.881, 1.616)	0.254	1.308 (0.98, 1.746)	**0.068***
Mean of positive pixels	0.966 (0.937, 0.995)	**0.024***	0.961 (0.926, 0.998)	**0.038***
SSF = 6 (coarse)				
Entropy	0.77 (0.27, 2.196)	0.624	1.068 (0.306, 3.73)	0.918
Mean intensity	1.002 (0.992, 1.012)	0.662	1.004 (0.991, 1.017)	0.571
Standard deviation	0.971 (0.943, 1.00)	**0.048***	0.978 (0.947, 1.01)	0.17
Skewness	0.801 (0.429, 1.494)	0.486	0.733 (0.356, 1.508)	0.398
Kurtosis	1.184 (0.937, 1.496)	0.158	1.22 (0.982, 1.516)	**0.072***
Mean of positive pixels	0.977 (0.952, 1.002)	**0.068***	0.976 (0.946, 1.006)	0.114

Note.—Data in parentheses are 95% confidence intervals.
* Indicates a significant difference ($p < 0.1$).

Table 5
Univariate Cox-Proportional Hazards Regression Analysis of Post-Treatment Tumor CT Texture Parameters for Progression-Free Survival and Overall Survival.

	Progression-Free Survival		Overall Survival	
Spatial scaling factor (SSF)	HR	P Value	HR	P Value
No filtration				
Entropy	2.584 (0.316, 21.13)	0.376	7.993 (0.506, 126.3)	0.140
Mean intensity	0.974 (0.949, 1.00)	**0.047***	0.96 (0.93, 0.991)	**0.012***
Standard deviation	1.041 (0.912, 1.187)	0.553	1.055 (0.91, 1.224)	0.476
Skewness	2.929 (0.973, 8.814)	**0.056***	1.935 (0.608, 6.153)	0.264
Kurtosis	0.934 (0.442, 1.975)	0.859	0.82 (0.364, 1.847)	0.632
Mean of positive pixels	0.973 (0.947, 1.00)	**0.049***	0.958 (0.926, 0.991)	**0.013***
SSF = 2 (fine)				
Entropy	1.021 (0.268, 3.889)	0.976	1.105 (0.275, 4.446)	0.888
Mean intensity	0.997 (0.988, 1.006)	0.505	1.00 (0.991, 1.01)	0.93
Standard deviation	1.00 (0.984, 1.017)	0.965	0.986 (0.958, 1.016)	0.356
Skewness	1.135 (0.663, 1.942)	0.645	1.40 (0.634, 3.093)	0.405
Kurtosis	1.013 (0.936, 1.096)	0.75	1.037 (0.921, 1.168)	0.546
Mean of positive pixels	0.987 (0.955, 1.02)	0.431	0.98 (0.942, 1.02)	0.316
SSF = 3 (medium)				
Entropy	0.976 (0.661, 1.44)	0.902	1.111 (0.30, 4.113)	0.874
Mean intensity	0.995 (0.986, 1.004)	0.29	0.999 (0.989, 1.009)	0.802
Standard deviation	0.997 (0.98, 1.013)	0.681	0.984 (0.956, 1.012)	0.246
Skewness	1.005 (0.766, 1.32)	0.969	0.895 (0.433, 1.852)	0.766
Kurtosis	1.009 (0.881, 1.154)	0.901	1.07 (0.903, 1.268)	0.432
Mean of positive pixels	0.983 (0.96, 1.008)	0.184	0.972 (0.939, 1.007)	0.115
SSF = 4 (medium)				
Entropy	1.142 (0.355, 3.676)	0.824	1.063 (0.324, 3.489)	0.92
Mean intensity	0.992 (0.98, 1.004)	0.172	0.993 (0.979, 1.007)	0.301
Standard deviation	0.994 (0.976, 1.012)	0.511	0.979 (0.95, 1.008)	0.147
Skewness	1.138 (0.612, 2.114)	0.683	0.825 (0.357, 1.904)	0.651
Kurtosis	1.101 (0.861, 1.408)	0.441	1.332 (0.975, 1.818)	**0.072***
Mean of positive pixels	0.985 (0.966, 1.005)	0.137	0.971 (0.942, 1.001)	**0.057***
SSF = 5 (coarse)				
Entropy	0.967 (0.346, 2.702)	0.949	0.892 (0.321, 2.481)	0.827
Mean intensity	0.991 (0.979, 1.003)	0.158	0.981 (0.961, 1.001)	**0.064***
Standard deviation	0.994 (0.977, 1.012)	0.52	0.977 (0.949, 1.007)	0.126
Skewness	1.744 (0.701, 4.337)	0.232	1.459 (0.433, 4.917)	0.542
Kurtosis	1.411 (0.955, 2.084)	**0.084***	2.083 (1.23, 3.527)	**0.006***
Mean of positive pixels	0.991 (0.977, 1.005)	0.194	0.975 (0.95, 1.00)	**0.05***
SSF = 6 (coarse)				
Entropy	1.001 (0.371, 2.705)	0.998	0.907 (0.328, 2.51)	0.851
Mean intensity	0.991 (0.98, 1.002)	0.114	0.978 (0.962, 0.995)	**0.013***
Standard deviation	0.991 (0.975, 1.007)	0.284	0.978 (0.952, 1.004)	**0.095***
Skewness	0.91 (0.464, 1.784)	0.783	1.219 (0.506, 2.94)	0.659
Kurtosis	0.923 (0.687, 1.24)	0.593	1.139 (0.834, 1.556)	0.413
Mean of positive pixels	0.991 (0.978, 1.003)	0.148	0.973 (0.95, 0.997)	**0.027***

Note.—Data in parentheses are 95% confidence intervals.
* Indicates a significant difference ($p < 0.1$).

4. Discussion

To date contrast-enhanced CT imaging is commonly used in the assessment of unresectable PDAC, and our results demonstrated that CT texture analysis could serve as a potential noninvasive biomarker for predicting survival.

Tumor size and other potential significant clinical parameters were included into multivariate model, and the results showed that tumor size, which is a determinant factor for the assessment of T stage, was associated with PFS (HR = 1.348; 95% CI: 1.081, 1.681; P = 0.008) and OS (HR = 1.35; 95% CI: 1.092, 1.669; P = 0.006). Furthermore, both pre-treatment tumor SD (HR = 0.942; 95% CI: 0.898, 0.988; P = 0.014) and skewness (HR = 0.407; 95% CI: 0.172, 0.962; P = 0.041) measured with SSF = 3, and tumor SD (HR = 0.958; 95% CI: 0.92, 0.997; P = 0.037) measured with SSF = 4 on contrast-enhanced CT images were associated with PFS in patients who planned to start definitive chemotherapy for unresectable PDAC. Meanwhile, pre-treatment tumor SD (HR = 0.928; 95% CI: 0.882, 0.976; P = 0.003) measured with SSF = 3 were also found to be significant prognostic factors for OS. Therefore, our results confirmed the fact that independent of the effects of tumor size, age and sex, tumor SD and skewness as continuous variables are independent predictors of survival.

According to these positive findings from multivariate models, Kaplan-Meier analysis was further performed and the results showed that tumor size was negatively associated with PFS and OS, which were consistent with expectations as TNM staging system was derived from survival analysis data. Higher SD, which suggest higher intratumoral heterogeneity before chemotherapy, were found to be significant positive prognostic factors for PFS and OS. Another result of Kaplan-Meier analysis showed that higher skewness was not significantly associated with better PFS, although our multivariate model had already proved that skewness was an independent predictor of survival. The most likely reason was that the result of Kaplan-Meier analysis was more susceptible to interference from mixed factors than multivariate analysis.

To date there have been few studies of texture analysis in PDAC. A previous single center retrospective study of 30 patients investigated the potential use of texture analysis in predicting OS in patients undergoing resection for PDCA [16]. In their results, less inverse difference normalized and greater dissimilarity are associated with longer OS. Yue et al. [22] assessed the prognostic value of PET/CT texture variations in predicting radiotherapy response of 26 PDCA patients. A total of 48 texture were identified and evaluated for association with OS in a multivariate model and finally 3 parameters including variations of

Table 6
Univariate Cox-Proportional Hazards Regression Analysis of Δ value (difference between posttreatment and pretreatment texture parameters) in Tumor CT Texture Parameters for Progression-Free Survival and Overall Survival.

	Progression-Free Survival		Overall Survival	
Spatial scaling factor (SSF)	HR	P Value	HR	P Value
No filtration				
Entropy	1.011 (0.761, 1.341)	0.937	0.78 (0.392, 1.55)	0.478
Mean intensity	0.991 (0.961, 1.002)	0.575	0.991 (0.959, 1.024)	0.592
Standard deviation	1.038 (0.944, 1.14)	0.443	1.024 (0.911, 1.15)	0.694
Skewness	1.063 (0.84, 1.346)	0.609	0.927 (0.629, 1.365)	0.700
Kurtosis	0.997 (0.769, 1.293)	0.983	0.866 (0.592, 1.267)	0.459
Mean of positive pixels	0.992 (0.96, 1.025)	0.617	0.991 (0.957, 1.026)	0.615
SSF = 2 (fine)				
Entropy	0.826 (0.248, 2.747)	0.755	0.813 (0.266, 2.485)	0.716
Mean intensity	0.997 (0.988, 1.005)	0.436	1.001 (0.991, 1.011)	0.898
Standard deviation	1.004 (0.986, 1.022)	0.702	0.989 (0.96, 1.019)	0.456
Skewness	1.033 (0.662, 1.612)	0.886	1.281 (0.767, 2.139)	0.345
Kurtosis	1.043 (0.995, 1.094)	**0.079***	1.01 (0.965, 1.057)	0.67
Mean of positive pixels	0.992 (0.96, 1.025)	0.691	0.993 (0.961, 1.026)	0.674
SSF = 3 (medium)				
Entropy	1.17 (0.333, 4.112)	0.807	1.168 (0.337, 4.052)	0.806
Mean intensity	0.995 (0.986, 1.003)	0.236	1.00 (0.989, 1.01)	0.938
Standard deviation	1.006 (0.991, 1.022)	0.437	0.998 (0.981, 1.016)	0.839
Skewness	1.158 (0.753, 1.781)	0.505	1.223 (0.766, 1.952)	0.399
Kurtosis	1.067 (0.987, 1.153)	0.103	1.019 (0.946, 1.097)	0.627
Mean of positive pixels	0.994 (0.972, 1.016)	0.596	0.996 (0.97, 1.023)	0.78
SSF = 4 (medium)				
Entropy	1.529 (0.477, 4.898)	0.474	1.307 (0.411, 4.155)	0.65
Mean intensity	0.991 (0.98, 1.003)	0.151	0.997 (0.984, 1.009)	0.594
Standard deviation	1.009 (0.994, 1.024)	0.243	0.999 (0.985, 1.014)	0.941
Skewness	1.235 (0.753, 2.024)	0.403	1.289 (0.73, 2.277)	0.381
Kurtosis	1.164 (0.954, 1.422)	0.135	1.063 (0.871, 1.296)	0.548
Mean of positive pixels	0.997 (0.982, 1.012)	0.688	0.997 (0.977, 1.017)	0.739
SSF = 5 (coarse)				
Entropy	1.468 (0.494, 4.361)	0.49	0.998 (0.354, 2.813)	0.996
Mean intensity	0.992 (0.981, 1.004)	0.195	0.995 (0.983, 1.007)	0.375
Standard deviation	1.009 (0.994, 1.025)	0.228	0.998 (0.982, 1.014)	0.793
Skewness	1.444 (0.776, 2.687)	0.247	1.725 (0.809, 3.675)	0.158
Kurtosis	1.139 (0.818, 1.588)	0.441	1.05 (0.70, 1.576)	0.814
Mean of positive pixels	0.997 (0.988, 1.007)	0.609	0.995 (0.98, 1.009)	0.471
SSF = 6 (coarse)				
Entropy	1.563 (0.549, 4.449)	0.403	0.894 (0.314, 2.546)	0.833
Mean intensity	0.994 (0.985, 1.003)	0.204	0.994 (0.983, 1.005)	0.257
Standard deviation	1.004 (0.989, 1.02)	0.617	0.994 (0.977, 1.011)	0.472
Skewness	1.005 (0.554, 1.826)	0.986	1.415 (0.684, 2.925)	0.349
Kurtosis	0.835 (0.649, 1.076)	0.163	0.856 (0.628, 1.167)	0.326
Mean of positive pixels	0.996 (0.987, 1.005)	0.395	0.991 (0.976, 1.006)	0.239

Note.—Data in parentheses are 95% confidence intervals.
* Indicates a significant difference ($p < 0.1$).

Table 7
Pre-Treatment Multivariate Cox-Proportional Hazards Regression Analysis.

	Progression-Free Survival		Overall Survival	
	HR	P Value	HR	P Value
Tumor size	1.348 (1.081, 1.681)	0.008	1.35 (1.092, 1.669)	0.006
SSF = 3 (medium)				
Standard deviation	0.942 (0.898, 0.988)	0.014	0.928 (0.882, 0.976)	0.003
Skewness	0.407 (0.172, 0.962)	0.041		
SSF = 4 (medium)				
Standard deviation	0.958 (0.92, 0.997)	0.037		

Note.—Data in parentheses are 95% confidence intervals and models were adjusted for age, sex, and tumor size (cm). *P* value less than 0.05 indicates a significant difference.

homogeneity, variance, and cluster tendency were found to be significant. Another retrospective study conducted by Chakraborty et al. [23] demonstrated 2-year prediction of survival of 35 patients who enrolled in a phase II clinical trial on the role of neoadjuvant chemotherapy in resectable PDAC using texture image features extracted from pre-treatment CT scans. They found that ACM1 and ACM2, which represent directional change in intensity of an image, achieved the best performance among all features.

In our study, SD has been demonstrated to be closely associated with both PFS and OS, and higher SD, which indicated higher intratumoral heterogeneity, predicted better survival outcome in patients with unresectable PDAC. However, in many cancers, increased tumor heterogeneity is associated with worse outcomes [24–26]. Hypoxia and necrosis, correlated with impaired response to chemotherapy and radiotherapy, are likely to occur in tumors with low levels of angiogenesis, which were closely associated with SD value. In addition, tumor necrosis, which can reflect the presence of hypoxia, was investigated by previous study to verify its significant value in predicting outcome in patients with PDAC, and multivariate survival analysis showed that necrosis was an independent predictor of poor outcome in terms of both disease-free survival (DFS) and disease-specific survival

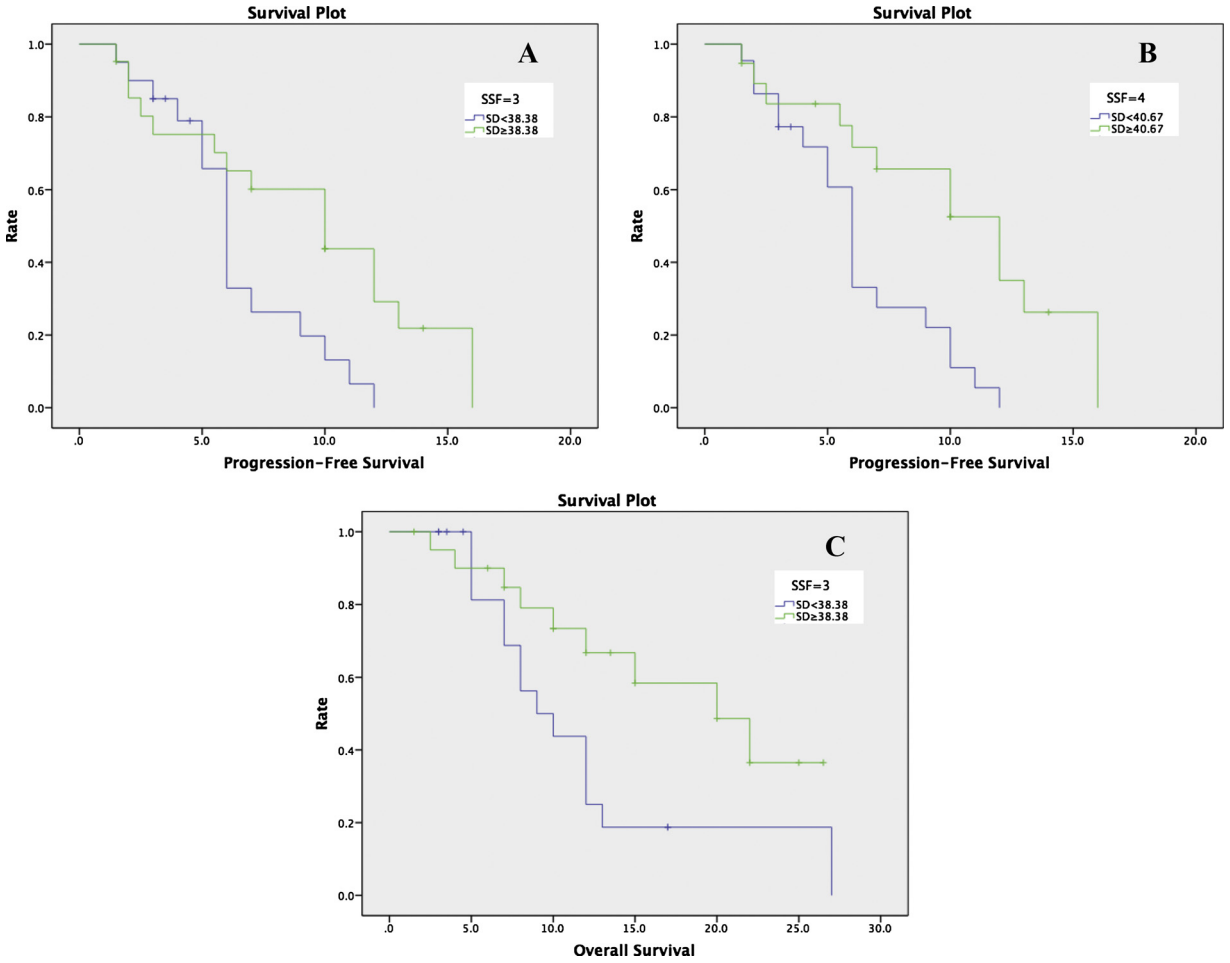

Fig. 2. Kaplan-Meier curves (log-rank test) of progression-free survival (a, b) and overall survival (c) according to tumor standard deviation (SD).

(DSS) of PDAC patients [27]. Nonetheless, contradictory results have also been reported; homogenous texture may represent higher cellular density or denser desmoplasia, which is thought to be closely associated with metastasis, as well as chemotherapy resistance, by reducing the amount of drug delivered to the tumor [28]. Consequently, behavior of the tumor becomes more aggressive. Hence, our conclusions are in accordance with those reported by Kim et al. [20] and Yun et al. [29], suggesting that PDAC may be an exception from the rule that tumor heterogeneity equals worse prognosis.

None of the post-therapy texture parameters or Δ value had a significant association with OS or PFS in our study. A possible explanation is that pretreatment texture parameters may provide additional information about baseline tumor biology, while posttreatment texture features may mainly reflect response to treatment. The use of chemotherapy in unresectable PDAC patients could have decreased the absolute and proportional texture changes, thus possibly covering the prognostic significance of these changes after treatment. In addition, small sample size in this study may also contribute to the difference.

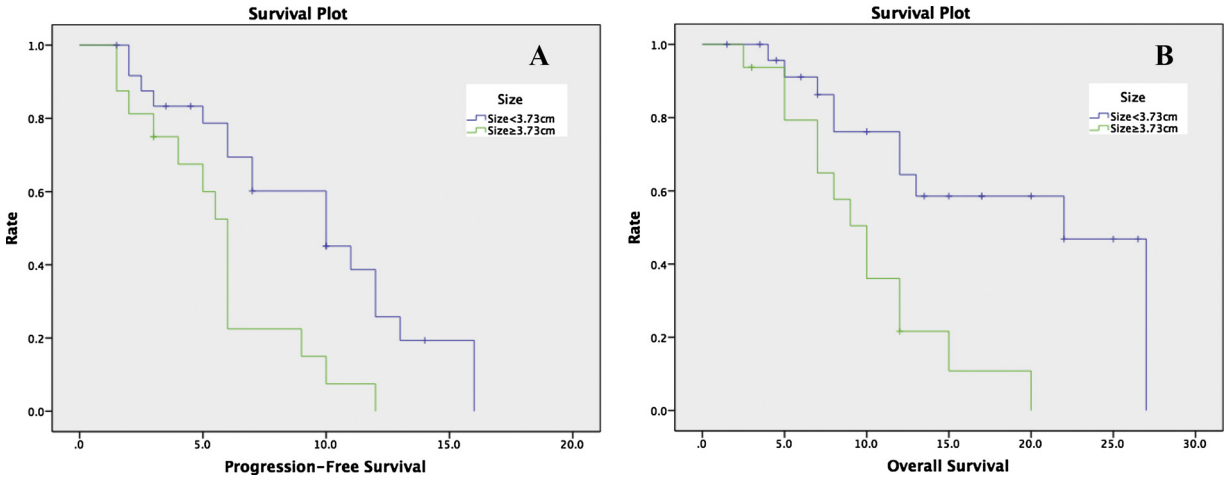

Fig. 3. Kaplan-Meier curves (log-rank test) of progression-free survival (a) and overall survival (b) according to tumor size.

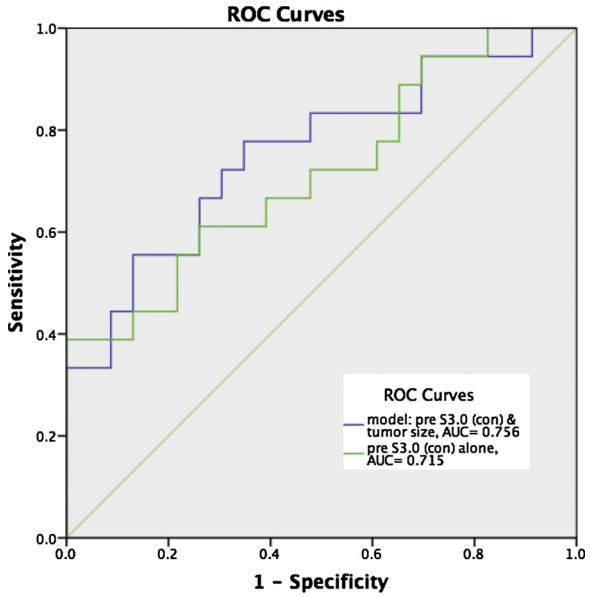

Fig. 4. Graph shows ROC curves of significant survival models. pre S3.0 (con) = pretreatment SD (filter 3.0) as continuous variable.

There is one very recent article by Sandrasegaran et al. [19] that has just been published with a significant overlap with our aims. However, methods and findings varied between these two studies. Their patients had chemotherapy and radiotherapy, while in our study, only chemotherapy were given, which could influence the prognosis of patients. In addition, patients included in our study were all histologically diagnosed of PDAC, while patients with different histological types of the pancreas might also be included in their population. Furthermore, we did not find texture parameters MPP or kurtosis to be associated with survival neither in multivariate analysis or Kaplan-Meier analysis, and metastatic disease at presentation had no significant association with OS or PFS in our study. Interestingly, tumor size was not significantly correlated with poor outcomes in their study, which was opposite to our result. These findings may be explained by differences of lesion location between our study and the previously published study. In our study, most patients had tumors in the body and tail of the pancreas, while 88% patients had cancer in the head of pancreas in previous study. Results might be quite different since not only tumors in body and tail tend to present later in the disease course, but also likely due to their more aggressive tumor biology [30]. Nevertheless, in the present study, no significant difference in PFS and OS was detected. Similarly, univariate Cox proportional hazards regression models were used by Bednar et al. [31] to study independent prognostic factors for OS in locally advanced unresectable pancreatic cancer, and tumor location (head/neck vs. body/tail) was not significantly associated with OS ($P = 0.077$). A possible explanation might be that compared with pancreatic cancer in the body and tail, patients with pancreatic cancer in the head were more prone to have various complications, as advanced tumors in the head often led to obstructive jaundice, impaired liver function, and invasion to the duodenum.

Notably, texture analysis was performed in the portal phase of the contrast enhanced CT in our present study according to previous studies [16,18–20]. Although Bronstein et al. [32] proved that the pancreatic phase was preferred to the portal phase, the quantitative assessment of McNulty et al. [33] found that tumor conspicuity is equivalent in the pancreatic and portal phases. Furthermore, during the portal phase, the progressive accumulation of contrast medium within the tumor might provide more comprehensive information of the biological characteristics of tumors. Thus, the above reasons might explain why portal phase was chosen by previous studies for texture analysis.

There are several limitations in our study. First of all, the time-independent ROC curve analysis was used in the assessment of survival models. As the duration of follow-up time varied, patients with censored data who were still stable or alive at the end of the follow-up period might be the consequence of insufficient follow-up time. Thus, instead of reflecting the global characteristics of survival, time-independent ROC curve could only reflect the situation of survival at a specific time point. Secondly, it was a retrospective study and the number of patients included in this study was limited. Furthermore, unresectable PDAC with locally advanced and those with distant metastasis should be separately discussed, as well as tumors in the body and tail and that in the head of the pancreas, in order to get more accurate results of the prognosis respectively in the future. However, the requirement of consistent chemotherapy plan and complete pretreatment and posttreatment CT imaging might make the formation of larger cohorts difficult. Thirdly, in this study, CT texture analysis was only performed on a single image which represent the largest area of the lesion. This may not exactly and comprehensively reflect disease characteristics, although prior studies reported that comparison of 2D vs. 3D measurements of single lesions showed fairly comparable results [34,35].

In conclusion, instead of post-chemotherapy texture parameters or Δ value, pre-chemotherapy could provide more information about tumor biology. Therefore, using pre-chemotherapy texture of unresectable PDAC to predict survival is more accurate and reliable. Furthermore, texture analysis as a noninvasive image-processing tool has the potential to select patients with good prognosis before therapy, indicating a promising prospect of clinical application in the future.

Conflicts of interest

All authors declare that they have no conflicts of interest to disclose.

Acknowledgements

The authors thank Danqin Yi and Dr. rodriguez.chapin for their editorial assistance and language revision in the preparation of this manuscript.

References

[1] R.L. Siegel, K.D. Miller, A. Jemal, Cancer statistics, CA Cancer J. Clin. 68 (2018) (2018) 7–30, https://doi.org/10.3322/caac.21442.
[2] A.V. Sheahan, A.V. Biankin, C.R. Parish, L.M. Khachigian, Targeted therapies in the management of locally advanced and metastatic pancreatic cancer: a systematic review, Oncotarget. 9 (2018) 21613–21627, https://doi.org/10.18632/oncotarget.25085.
[3] R.D.A. Peixoto, C. Speers, C.E. Mcgahan, D.J. Renouf, D.F. Schaeffer, H.F. Kennecke, Prognostic factors and sites of metastasis in unresectable locally advanced pancreatic cancer, Cancer Med. (2015), https://doi.org/10.1002/cam4.459.
[4] J. Tabernero, E.G. Chiorean, J.R. Infante, S.R. Hingorani, V. Ganju, C. Weekes, W. Scheithauer, R.K. Ramanathan, D. Goldstein, D.N. Penenberg, A. Romano, S. Ferrara, D.D. Von Hoff, Prognostic factors of survival in a randomized phase III trial (MPACT) of weekly nab-paclitaxel plus gemcitabine versus gemcitabine alone in patients with metastatic pancreatic cancer, Oncologist. (2015), https://doi.org/10.1634/theoncologist.2014-0394.
[5] E. Giovannetti, Q. Wang, A. Avan, N. Funel, T. Lagerweij, J.H. Lee, V. Caretti, A. Van Der Velde, U. Boggi, Y. Wang, E. Vasile, G.J. Peters, T. Wurdinger, G. Giaccone, Role of CYB5A in pancreatic cancer prognosis and autophagy modulation, J. Natl. Cancer Inst. (2014), https://doi.org/10.1093/jnci/djt346.
[6] J. Han, F. Wang, S. qiang Yuan, Y. Guo, Z. lei Zeng, L. ren Li, J. Yang, D. sen Wang, M. yuan Liu, H. Zhao, K. yan Liu, J. wei Liao, Q. feng Zou, R. hua Xu, Reduced expression of p21-activated protein kinase 1 correlates with poor histological differentiation in pancreatic cancer, BMC Cancer (2014), https://doi.org/10.1186/1471-2407-14-650.
[7] H. Li, X. Wang, C. Wen, Z. Huo, W. Wang, Q. Zhan, D. Cheng, H. Chen, X. Deng, C. Peng, B. Shen, Long noncoding RNA NORAD, a novel competing endogenous RNA, enhances the hypoxia-induced epithelial-mesenchymal transition to promote metastasis in pancreatic cancer, Mol. Cancer (2017), https://doi.org/10.1186/s12943-017-0738-0.
[8] J. Zhou, S. Song, D. Li, S. He, B. Zhang, Z. Wang, X. Zhu, Decoy receptor 3 (DcR3) overexpression predicts the prognosis and pN2 in pancreatic head carcinoma, World J. Surg. Oncol. (2014), https://doi.org/10.1186/1477-7819-12-52.

[9] D.G. Duda, R.K. Jain, C.G. Willett, Antiangiogenics: the potential role of integrating this novel treatment modality with chemoradiation for solid cancers, J. Clin. Oncol. (2007), https://doi.org/10.1200/JCO.2007.11.3985.
[10] B. Ganeshan, K. Burnand, R. Young, C. Chatwin, K. Miles, Dynamic contrast-enhanced texture analysis of the liver: initial assessment in colorectal cancer, Invest. Radiol. (2011), https://doi.org/10.1097/RLI.0b013e3181f8e8a2.
[11] G. Castellano, L. Bonilha, L.M. Li, F. Cendes, Texture analysis of medical images, Clin. Radiol. (2004), https://doi.org/10.1016/j.crad.2004.07.008.
[12] F. Davnall, C.S.P. Yip, G. Ljungqvist, M. Selmi, F. Ng, B. Sanghera, B. Ganeshan, K.A. Miles, G.J. Cook, V. Goh, Assessment of tumor heterogeneity: An emerging imaging tool for clinical practice? Insights Imaging (2012), https://doi.org/10.1007/s13244-012-0196-6.
[13] B. Ganeshan, K.A. Miles, R.C.D. Young, C.R. Chatwin, H.M.D. Gurling, H.D. Critchley, Three-dimensional textural analysis of brain images reveals distributed grey-matter abnormalities in schizophrenia, Eur. Radiol. (2010), https://doi.org/10.1007/s00330-009-1605-1.
[14] B. Ganeshan, V. Goh, H.C. Mandeville, Q.S. Ng, P.J. Hoskin, K.A. Miles, Non–small cell lung Cancer: histopathologic correlates for texture parameters at CT, Radiology. (2013), https://doi.org/10.1148/radiol.12112428.
[15] C.G. Chee, Y.H. Kim, K.H. Lee, Y.J. Lee, J.H. Park, H.S. Lee, S. Ahn, B. Kim, CT texture analysis in patients with locally advanced rectal cancer treated with neoadjuvant chemoradiotherapy: a potential imaging biomarker for treatment response and prognosis, PLoS One (2017), https://doi.org/10.1371/journal.pone.0182883.
[16] A. Eilaghi, S. Baig, Y. Zhang, J. Zhang, P. Karanicolas, S. Gallinger, F. Khalvati, M.A. Haider, CT texture features are associated with overall survival in pancreatic ductal adenocarcinoma - a quantitative analysis, BMC Med. Imaging (2017), https://doi.org/10.1186/s12880-017-0209-5.
[17] M.B. Amin, F.L. Greene, S.B. Edge, C.C. Compton, J.E. Gershenwald, R.K. Brookland, L. Meyer, D.M. Gress, D.R. Byrd, D.P. Winchester, The Eighth Edition AJCC Cancer staging Manual: continuing to build a bridge from a population-based to a more “personalized” approach to cancer staging, CA Cancer J. Clin. (2017), https://doi.org/10.3322/caac.21388.
[18] C. Cassinotto, J. Chong, G. Zogopoulos, C. Reinhold, L. Chiche, J.P. Lafourcade, A. Cuggia, E. Terrebonne, A. Dohan, B. Gallix, Resectable pancreatic adenocarcinoma: role of CT quantitative imaging biomarkers for predicting pathology and patient outcomes, Eur. J. Radiol. (2017), https://doi.org/10.1016/j.ejrad.2017.02.033.
[19] K. Sandrasegaran, Y. Lin, M. Asare-Sawiri, T. Taiyini, M. Tann, CT texture analysis of pancreatic cancer, Eur. Radiol. (2018), https://doi.org/10.1007/s00330-018-5662-1.
[20] B.R. Kim, J.H. Kim, S.J. Ahn, I. Joo, S.Y. Choi, S.J. Park, J.K. Han, CT prediction of resectability and prognosis in patients with pancreatic ductal adenocarcinoma after neoadjuvant treatment using image findings and texture analysis, Eur. Radiol. (2018), https://doi.org/10.1007/s00330-018-5574-0.
[21] E.R. DeLong, D.M. DeLong, D.L. Clarke-Pearson, Comparing the areas under two or more correlated receiver operating characteristic curves: a nonparametric approach, Biometrics. (1988), https://doi.org/10.2307/2531595.
[22] Y. Yue, A. Osipov, B. Fraass, H. Sandler, X. Zhang, N. Nissen, A. Hendifar, R. Tuli, Identifying prognostic intratumor heterogeneity using pre- and post-radiotherapy 18F-FDG PET images for pancreatic cancer patients, J. Gastrointest. Oncol. (2017), https://doi.org/10.21037/jgo.2016.12.04.
[23] J. Chakraborty, L. Langdon-Embry, K.M. Cunanan, J.G. Escalon, P.J. Allen, M.A. Lowery, E.M. O’Reilly, M. Gönen, R.G. Do, A.L. Simpson, Preliminary study of tumor heterogeneity in imaging predicts two year survival in pancreatic cancer patients, PLoS One (2017), https://doi.org/10.1371/journal.pone.0188022.
[24] C. Yip, D. Landau, R. Kozarski, B. Ganeshan, R. Thomas, A. Michaelidou, V. Goh, Primary esophageal Cancer: heterogeneity as potential prognostic biomarker in patients treated with definitive chemotherapy and radiation therapy, Radiology. (2014), https://doi.org/10.1148/radiol.13122869.
[25] H. Zhang, C.M. Graham, O. Elci, M.E. Griswold, X. Zhang, M.A. Khan, K. Pitman, J.J. Caudell, R.D. Hamilton, B. Ganeshan, A.D. Smith, Locally advanced squamous cell carcinoma of the head and neck: CT texture and histogram analysis allow independent prediction of overall survival in patients treated with induction chemotherapy, Radiology. (2013), https://doi.org/10.1148/radiol.13130110.
[26] B. Ganeshan, E. Panayiotou, K. Burnand, S. Dizdarevic, K. Miles, Tumour heterogeneity in non-small cell lung carcinoma assessed by CT texture analysis: a potential marker of survival, Eur. Radiol. (2012), https://doi.org/10.1007/s00330-011-2319-8.
[27] N. Hiraoka, Y. Ino, S. Sekine, H. Tsuda, K. Shimada, T. Kosuge, J. Zavada, M. Yoshida, K. Yamada, T. Koyama, Y. Kanai, Tumour necrosis is a postoperative prognostic marker for pancreatic cancer patients with a high interobserver reproducibility in histological evaluation, Br. J. Cancer (2010), https://doi.org/10.1038/sj.bjc.6605854.
[28] X. Li, Q. Ma, Q. Xu, W. Duan, J. Lei, E. Wu, Targeting the cancer-stroma interaction: a potential approach for pancreatic Cancer treatment, Curr. Pharm. Des. (2012), https://doi.org/10.2174/13816128112092404.
[29] G. Yun, Y.H. Kim, Y.J. Lee, B. Kim, J.H. Hwang, D.J. Choi, Tumor heterogeneity of pancreas head cancer assessed by CT texture analysis: association with survival outcomes after curative resection, Sci. Rep. 8 (2018) 1–10, https://doi.org/10.1038/s41598-018-25627-x.
[30] S.B. Dreyer, N.B. Jamieson, R. Upstill-Goddard, P.J. Bailey, C.J. McKay, A.V. Biankin, D.K. Chang, Defining the molecular pathology of pancreatic body and tail adenocarcinoma, Br. J. Surg. (2018), https://doi.org/10.1002/bjs.10772.
[31] F. Bednar, M.S. Zenati, J. Steve, S. Winters, L.M. Ocuin, N. Bahary, M.E. Hogg, H.J. Zeh, A.H. Zureikat, Analysis of predictors of resection and survival in locally advanced stage iii pancreatic cancer: does the nature of chemotherapy regimen influence outcomes? Ann. Surg. Oncol. 24 (2017) 1406–1413, https://doi.org/10.1245/s10434-016-5707-0.
[32] Y.L. Bronstein, E.M. Loyer, H. Kaur, H. Choi, C. David, R.A. DuBrow, L.D. Broemeling, K.R. Cleary, C. Charnsangavej, Detection of small pancreatic tumors with multiphasic helical CT, Am. J. Roentgenol. (2004), https://doi.org/10.2214/ajr.182.3.1820619.
[33] N.J. McNulty, I.R. Francis, J.F. Platt, R.H. Cohan, M. Korobkin, A. Gebremariam, Multi–detector row helical CT of the pancreas: effect of contrast-enhanced multiphasic imaging on enhancement of the pancreas, peripancreatic vasculature, and pancreatic adenocarcinoma, Radiology (2001), https://doi.org/10.1148/radiology.220.1.r01jl1897.
[34] F. Ng, R. Kozarski, B. Ganeshan, V. Goh, Assessment of tumor heterogeneity by CT texture analysis: can the largest cross-sectional area be used as an alternative to whole tumor analysis? Eur. J. Radiol. (2013), https://doi.org/10.1016/j.ejrad.2012.10.023.
[35] S.J. Ahn, J.H. Kim, S.J. Park, J.K. Han, Prediction of the therapeutic response after FOLFOX and FOLFIRI treatment for patients with liver metastasis from colorectal cancer using computerized CT texture analysis, Eur. J. Radiol. (2016), https://doi.org/10.1016/j.ejrad.2016.08.014.